On Accurate Detection of Oceanic Features from Satellite IR Data Using ICSED Method

Li Jun (李 俊) and *Zhou Fengxian* (周凤仙)
Institute of Atmospheric Physics, Academia Sinica, Beijing 100029
Received September 29, 1991; revised November 28, 1991

ABSTRACT

ICSED (Improved Cluster Shade Edge Detection) algorithm and other various methods to accurately and efficiently detect edges on satellite data are presented. Error rate criterion is used to statistically evaluate the performances of these methods in detecting oceanic features for both noise free and noise contaminated AVHRR (Advanced Very High Resolution Radiometer) IR image with Kuroshio. Also, practical experiments in detecting the eddy of Kuroshio with these methods are carried out for comparison. Results show that the ICSED algorithm has more advantages than other methods in detecting mesoscale features of ocean. Finally, the effectiveness of window size of ICSED method to oceanic features detection is quantitatively discussed.

I. INTRODUCTION

The accurate detection of mesoscale features observed on satellite IR data is of interest to a wide range of disciplines. For example, oceanographers have used NOAA / AVHRR images to investigate mesoscale eddies (Simpson et al., 1984; Koblinsky et al., 1984), coastal filaments (Flamant et al.,1985) and open ocean frontal structure (Van Woert, 1982). The visual primitive of importance for many of these applications is the brightness gradient. Brightness gradient can be computed by using three different types of convolution operators: gradient operators, edge detectors, and edge enhancers. Gradient operators are used when the actual values of the brightness gradient are needed. Initialization and updating of numerical models with geophysical variables require such information. Edge detectors are used when only an accurate determination of the location of the feature boundary is needed. Computation of the normal component of near-surface oceanic velocity (Wahl and Simpson, 1990) and some commercial and / or sports fishing applications (Svejkovsky, 1988) often use edge detectors. Edge enhancers are used to increase the signal-to-noise ratio of a feature that is only weakly visible on a parent image (Simpson et al., 1990).

The most common image edge operators are based on approximation of the intensity gradient on the image. The two-dimensional brightness gradient is defined as

$$\nabla g = \frac{\partial g}{\partial x}\vec{i} + \frac{\partial g}{\partial y}\vec{j}\ , \tag{1}$$

where $g(x,y)$ is the brightness temperature of the image. ∇g measures a local maximum in the direction of an edge . The direction of the edge, θ, is determined by the relation

$$\theta = \arctan\left[\frac{\partial g / \partial y}{\partial g / \partial x}\right] \tag{2}$$

and the magnitude of the gradient is defined as

$$|\nabla g| = \left[\left(\frac{\partial g}{\partial x}\right)^2 + \left(\frac{\partial g}{\partial y}\right)^2\right]^{\frac{1}{2}} . \tag{3}$$

A computationally more efficient way to calculate the magnitude of the gradient is the approximation

$$|\nabla g| = \left|\frac{\partial g}{\partial x}\right| + \left|\frac{\partial g}{\partial y}\right| . \tag{4}$$

The convolution operators most commonly used to compute two-dimensional gradients are given in Table 1. The edge detection algorithm ICSED method put forward by Li (1990) is based on the cluster shade texture measurement. It is derived from Gray Level Co-occurrence (GLC). GLC matrix has been used to investigate edge measurement of Gulf stream (Holyer et al., 1989) and Kuroshio (Li et al., 1990). The ICSED method is done by computing $S(0,0)$ (Li et al., 1990) in a $M \times N$ pixel image or local neighborhood within an image with L intensity levels ranging from 0 to $L-1$ as follows

$$S(0,0) = \frac{1}{MN}\sum_{m=1}^{M}\sum_{n=1}^{N}(g(m,n) - \mu)^k , \qquad k = 3.5.7\cdots \tag{5}$$

where $g(m,n)$ denotes the intensity level of the pixel at line m, and element n, and

$$\mu = \frac{1}{MN}\sum_{m=1}^{M}\sum_{n=1}^{N}(g(m,n)) .$$

Then the edges can be detected by finding the significant zero crossings on the cluster shade image $S(0,0)$.

Table 1. Commonly Used Edge Operators

	g_x	g_y
Roberts	$\begin{bmatrix} 0 & 1 \\ -1 & 0 \end{bmatrix}$	$\begin{bmatrix} 1 & 0 \\ 0 & -1 \end{bmatrix}$
Sobel	$\begin{bmatrix} -1 & 0 & 1 \\ -2 & 0 & 2 \\ -1 & 0 & 1 \end{bmatrix}$	$\begin{bmatrix} -1 & -2 & -1 \\ 0 & 0 & 0 \\ 1 & 2 & 1 \end{bmatrix}$
Isotropic	$\begin{bmatrix} -1 & 0 & 1 \\ -\sqrt{2} & 0 & \sqrt{2} \\ -1 & 0 & 1 \end{bmatrix}$	$\begin{bmatrix} -1 & -\sqrt{2} & -1 \\ 0 & 0 & 0 \\ 1 & \sqrt{2} & 1 \end{bmatrix}$
Kirsch	$\begin{bmatrix} -3 & -3 & 5 \\ -3 & 0 & 5 \\ -3 & -3 & 5 \end{bmatrix}$	$\begin{bmatrix} 5 & 5 & 5 \\ -3 & 0 & -3 \\ -3 & -3 & -3 \end{bmatrix}$

This paper quantitatively examines ICSED algorithm and other methods in detecting edges from satellite IR image. In general, cloud contamination can often be a serious error source in edge detection because the noise introduced by clouds is preferentially amplified by the edge operators. Good noise rejection edge detector must be selected in order to identify mesoscale features effectively. On the other hand, delineation of mesoscale features of ocean

requires the most effective edge detector which exhibits the characteristic of fine-structure rejection while retaining edge sharpness. This characteristic is highly desirable for analyzing oceanographic satellite images. Therefore, testing and selecting an excellent edge detector are very significant to analyze the oceanographic satellite data and other satellite images.

In order to evaluate the performance of popular edge operators and ICSED algorithm, and the effectiveness of window size M and N to ICSED method in detecting oceanic features testing examination was done by adding noise to the parent image. Numerical measures of successful noise rejection are introduced to determine that ICSED method is least sensitive to geophysical noise in satellite data. They are also used to quantitatively intercompare the performancs of various edge operators. On the other hand, practical experiments in detecting the eddy of Kuroshio from NOAA / AVHRR IR image with ICSED algorithm and other detection methods are carried out for comparison. It shows that ICSED method has the characteristic of rejecting weak gradients while keeps the main edge sharpness comparing with other detectors. Final recommendation is made for ICSED algorithm with proper window size M and N suited to the analysis of oceanic features on satellite data.

II. IMAGES

1. *Parent Image*

A 256 × 256 pixel AVHRR IR image (Channel 4) taken on 5 March 1986 with 8-bit accuracy and 1.8 km spatial resolution was used in this study. The AVHRR data were received at the Remote Sensing Division, National Research Center for Marine Environment Forecasts. The image shows the mesoscale features of Kuroshio such as meander and scope.

2. *Synthetic Image*

Synthetic image was created from the parent image in order to objectively determine the effectiveness of each operator when the input image was contaminated with noise. First, the standard deviation of the parent image was determined. Then, Gaussian white noise images with zero means and standard deviations of 2%, 5%, 10% and 20% of the given parent image's standard deviation were created. These noise images were then added to the parent image to produce noise-corrupted version of the parent image. It is noted that the synthetic images so produced are perfectly coregistered with the parent image. In our study Gaussian noise is chosen to evaluate ICSED algorithm and other edge detectors because Gaussian noise is mathematically well represented and understood.

III. STATISTICAL EVALUATION OF ICSED METHOD AND OTHER EDGE DETECTORS

1. *Method*

Statistical error functions were used to objectively evaluate the performance of each operator (ICESD, Sobel, Kirsch, Roberts, Isotropic) on NOAA / AVHRR IR image. The two error functions (Jain, 1989) are:

$$P_e = \frac{N_d}{N_i} \quad , \tag{6}$$

$$P_e = \frac{1}{\max(N_i, N_d)} \sum_{i=1}^{N_d} \frac{1}{1 + \alpha g_i^2} \quad , \tag{7}$$

where N_i is the number of pixels on an ideal edge and N_d is the number of pixels on a detected edge, g_i is the distance between a pixel and its nearest ideal edge pixel, and α is a calibration constant. For perfectly coregistered images, $\alpha = 1$. Note that both Eq.(6) and Eq.(7) equal 1 when the detected edge is identical to the ideal edge. Here we use Eq.(6) for the sake of convenience.

Use of Eq.(6) to evaluate the performance of edge detectors in the presence of noise requires the construction of "ideal" and "detected" edge images for each operator. To insure a statistically large enough population for operator evaluation, a 2500–pixel parent ideal edge mask was created for each operator from the parent image. For this purpose the threshold value of the top 2500 pixels was computed from the cumulative histogram of the parent gradient image or cluster shade image. This threshold value was used to create a parent edge mask as ideal with 2500 pixels having value '1' and all other pixel values are set to '0'. The same threshold value was used to map pixels in the corresponding synthetic gradient images to a "detected" edge mask with '1' and '0'. Edge masks for the synthetic images often have much more "detected" edges comparing with their "ideal" equivalence because the added noise generally causes the operators to detect a larger number of anomalously high gradients.

2. *Results*

The performace of each edge operator (Isotropic, Sobel, Kirsch, Roberts and ICSED) on the parent image and on the 2%, 5%, 10% and 20% rms noise–contaminated synthetic images was objectively determined using Eq.(6). The results have been synthesized into a single figure which shows the number of edge pixels detected by each operator as a function of percent rms noise added to the parent image (Fig. 1). The pixel number of ideal edges on the noisefree parent image was set to 2500, all operators perform about equally well for 0%, 2% and 5% noise contamination. With 10% noise all operators except ICSED detect more than 3500 edge pixels. With 20% noise, Isotropic, Sobel, Kirsch and Roberts begin to detect a large number of erroneous edges while ICESD still detects relatively smaller additional edges comparing with those edge operators. The performance of five operators on the parent image and on the noise–contaminated synthetic images produced from the parent image was objectively evaluated using error rate criterion [Eq.(6)]. With increasing levels of rms Gaussian noise the ICSED method performed better than all other operators. Even at 20% rms Gaussian noise, the ICSED technique still does well on effectiveness of noise rejection than other operators.

Table 2. Values of P_ε Computed Using Eq.(6) as a Function of Gaussian Noise Added to Parent Image and Edge Operators

Gaussian Noise	2%	5%	10%	20%
Isotropic	1.003	1.007	1.457	4.182
Sobel	1.002	1.005	1.540	4.524
Kirsch	1.002	1.004	1.687	4.594
Roberts	1.021	1.059	4.034	10.584
ICSED (k = 5)	1.000	1.001	1.112	2.629

Eqs.(6) and (7) provide quantitative means for evaluating the ability of each gradient operator to properly detect edges in the presence of noise. When a detected edge is identical to an ideal edges, then both Eqs.(6) and (7) equal 1. If the number of detected edges exceeds the

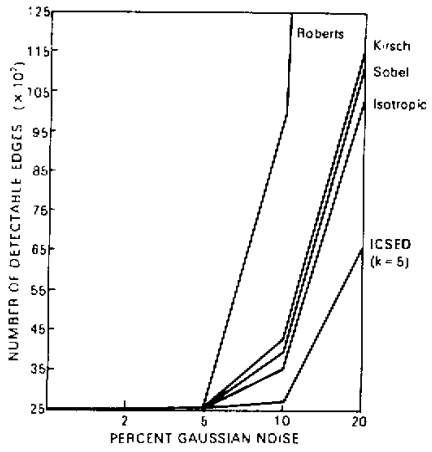

Fig.1. Plots of the pixel number of edges detected by each edge operator as a function of percentage of rms Gaussian noise added to the parent image.

number of ideal edges, then the value of P_e calculated from Eq.(6) will exceed 1, while its value calculated from Eq.(7) will approach 0. Values of P_e (shown in Table 2) as a function of Gaussian noise contamination and gradient operator for the parent image indicate that, of the group of edge operators tested, the best overall operator in the presence of noise is the ICSED.

IV. PRACTICAL EXPERIMENTS IN DETECTING EDDY OF KUROSHIO

In order to compare the performances of ICSED algorithm and other methods, the NOAA / AVHRR IR image with eddy of Kuroshio is used for experiments. The cloud cover was removed by use of dynamic clustering technique (Li et al., 1990) before applying the edge operators to the image. Testing results are compared and analyzed between ICSED algorithm and other methods.

The popular edge detectors, based on first derivative, share a common shortcoming in the present application. Namely, they are too sensitive to noise, to fine-structure of the edges, and to weak gradients. To illustrate this problem, the g_x and g_y of Sobel, Isotropic, Kirsch and Roberts, selected as typical of the 3×3 kernel (Roberts 2×2) derivative appoximation methods, have been applied to the parent image, and the gradient magnitude has been calculated using Eq.(3). Fig. 2 is an image of Sobel gradient values, Fig. 3 the Isotropic, Fig.4 the Kirsch and Fig.5 the Roberts. The mesoscale features have been captured on the IR image by applying four edge operators, but many areas of the image free of mesoscale structure also exhibit edges comparable to those contained within the mesoscale features. Furthermore, the edges within the mesoscale features are very complex structures that show great details. In many applications these enhancements of details by the edge operators are desirable. However, a preferable result in detecting the oceanic features would be an edge operator that resulted in simple, smooth representations of edges within the mesoscale features and no edge at all in the oceanographically blank areas of the image. Of course, the derivative-based edge operators could be made less sensitive to details and weak edges by increasing the size of the convolution kernel used to estimate the derivatives. However, larger kernels produce a "blurring", which results in edges that are broad blanks rather than sharp boundaries.

The ICSED algorithm is based on the cluster shade texture, which is derived from the

Gray Level Co-occurrence (GLC) matrix, and the edges could be detected by finding the significant zero crossings on the cluster shade image. Because edges are detected by finding zero crossings, precisely positioned lines result in even if the GLC matrix is calculated over a large window. (The lines are formed in two-pixel width because the zero crossing algorithm detects both the large positive value with a large negative neighbor and the large negative value with a large positive neighbor.) The improved cluster shade edge detector, therefore, does not give blurred or positionally uncertain edges when large windows are used. The desired edge detection characteristics of retaining sharp edges while eliminating edge details are thereby achieved. In addition to setting the window size to reject edge details, the threshold used to determine which zero crossings are significant can also be adjusted to eliminate weak edges, and the exponent k could be set large enough in order to retain edge sharpness. Therefore, three major tunable parameters are associated with this algorithm. Fig.6 illustrates the eddy of Kuroshio using ICSED method with window size $M = N = 9$, and exponent $k = 5$. It is obvious from the edge image that this algorithm has the characteristics of smoothing the fine structure in the edges while preserving edge sharpness and accurate localization comparing with the popular edge operators such as Sobel, Isotropic, Kirsch, Roberts etc.

Fig.2. Result of applying the Sobel edge operator.

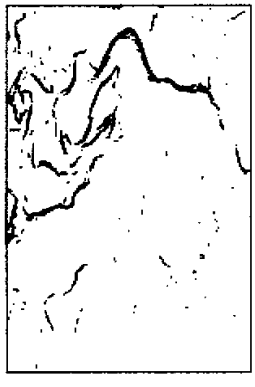

Fig.3. Result of applying the Isotropic edge operator.

Fig.4. Result of applying the Kirsch edge operator.

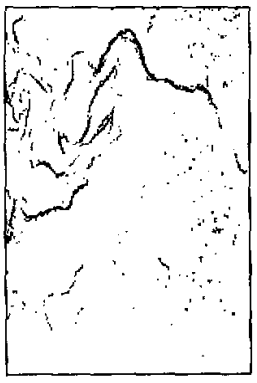

Fig.5. Result of applying the Roberts edge operator.

Fig.6. Application of ICSED method with $k = 5$, $M = N = 9$.

V. THE RELATION BETWEEN NOISE REJECTION AND CHOICE OF WINDOW SIZE M

Optimal window size should consider both quality of edges and the computational cost. Here result is presented which shows the relation between noise rejection and choice of window size M and N (for simplicity, $M = N$ is assumed in this paper).

The ability of the ICSED algorithm with a specific window size to accurately detect edges in noise contaminated image was tested using synthetic version of the parent image. This synthetic image was produced by adding 10% rms Gaussian noise to the parent image. Results for the synthetic image with 10% noise contamination using $M = 5,7,9,11,13$ and 15 show that for small window the added noise produces more erroneous edges. For $M \geqslant 7$, however, the erroneous edges are significantly reduced, and they are reached the minimum when $M = 15$. Fig.7 shows the plots of the number of edges detected by ICSED as a function of the window size on the synthetic image with 10% noise added. This result is consistent with

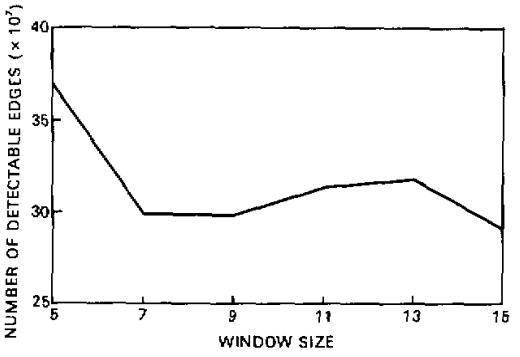

Fig.7. Plots of the number of edges detected by ICSED as a function of the window size on the synthetic image with 10% noise added.

theprevious choice $M = 9$ (Li et al., 1990). In general, the question of optimal window size is associated with the application and the spatial and temperal resolution of the image. To the small size window ICSED performs less noise rejection. With large size window, it has the characteristic of noise rejection but spends more computer time. So the medium size window gives the best result when considering both the quality of edges and the computational efficiency.

VI. DISCUSSION

1. *General Consideration*

Edge detection serves to simplify the analysis of images by significantly reducing the amount of data processed, while at the same time preserving useful structural information about object boundaries (Canny, 1986). Regardless of application, there are a few common criteria relevant to the performance measurement of all edge detectors. First, the error rate must be low. That is, edges that occur on the image should be detected. The second general criterion is that the edge points should be well localized. That is, the distance between the points marked by the detector and the "center" of the true edge should be minimized. An alternate interpretation of the localization constraint is that contributions to each point in the filtered image should arise from a smoothed average of nearby points, rather than any kind of average of widely scattered points (Marr and Hildreth, 1980). In present application, another requirement is that the edge operator should result in simple, smooth representations of edge within the mesoscale features and no edges at all in the oceanographically blank areas of an image. These general criteria provide the basis for the performance evaluation of all the operators used in this paper.

2. *Special Consideration*

In the laboratory, image acquisition is done under optimal conditions. In contrast, remotely-sensed images are often obtained under conditions 1) poor and non-uniform illumination, 2) poor viewing geometry, 3) atmospheric contamination, 4) reduced dynamic range in the domain of interest (e.g., ocean or land) resulting from images simultaneously containing cloud, land and ocean. Because these uncontrollable (at time of data acquisition) circumstances can significantly alter the effectiveness of any edge detector, it comes necessary to eliminate all such sources of "noise" from the image perior to edge analysis, these procedures include good cloud-screen, land-recognition (Li et al., 1990) etc.

3. *Application*

Detecting the mesoscale features of ocean is useful in guiding in near real-time oceanographic experiments, commercial fishing, and rescue operations. It can also be used to trace the dispersal patterns of marine pollutants (e.g., oil slicks and outfalls from waste treatment plants), and can be combined with other analysis procedures to help separating snow and ice from cloud on satellite data. Both real-time experiments and rescue operations require precise location information. The ICSED algorithm provides a computationally efficient way to produce this type of information. Finally, it should be noted that this technique is not limited to AVHRR data. It could be equally well used with LANDSAT data to study a broad range of terrestrial based problems, with CZCS data to study biological processes in the ocean, or using SSMR data to study ice flows and ice dynamics.

VII. CONCLUSIONS

The ICSED algorithm and a number of other edge operators to detect mesoscale features on remotely-sensed image are presented. Their performance is statistically evaluated for both noisefree and noisecontaminated images using error criterion. Also, practical experiments in detecting the eddy of Kuroshio from NOAA / AVHRR IR image with ICSED algorithm and other detection methods are carried out for comparison. Conclusions are drawn that ICSED method has the characteristics of good noise rejection, weak gradient rejection, and keeping the main edge sharpness comparing with other detectors such as Sobel, Isotropic, Kirsch, Roberts etc. in detecting oceanic features on satellite data. Finally, the proper window size of ICSED is recommended in present application.

We are grateful to the Remote Sensing Division, National Research Center for Marine Environment Forecasts for their providing the AVHRR images. We also wish to express our sincere thanks to Ms. Wu Wenhua for her help in this research program.

REFERENCES

Canny, J. (1986), A Computational Approach to Edge Detection, *IEEE Trans. Pattern Anal. Mach. Intelligence*, **6**: 679–698.

Cayula, J. F., P. Cornillon, R.Holyer and S.Peckinpaugh (1991), Comparative Study of Two Recent Edge-Detection Algorithms Designed to Process Sea-Surface Temperature Fields, *IEEE Trans. on Geoscience and Remote Sensing*, **29**: 175–177.

Cornillon, P. et al. (1988), Processing, Compression and Transmission of Satellite IR Data for NearReal-Time Use at Sea, *J. of Atmos. and Ocean Tech.*, **5**: 320–327.

Flament, P., L.Armi and L. Washburn (1985), The evolving structure of an upwelling filament, *J. Geophys. Res.* **90**: 11767–11778.

Gerson, D. J. and P. Gaborski (1977), Pattern analysis for automatic location of oceanic fronts in digital satellite imagery, Naval Oceanographic Office, TN 3700–65–77, Oct.

Hoyler, R. J. and S. H. Peckinpaugh (1989), Edge detection applied to satellite IR imagery of the ocean, *IEEE. Trans. Geosci. Remote Sensing*, **GE-27**: 46–56.

Janowitz, M. F. (1985), Automatic Detection of Gulf Stream. Office of Naval Research, Tech. Rep, TR-J8501, contr. N-00014-79-c-0629, June.

Kelly, K. A, (1985), Separating Clouds from Ocean in IR Images. *Remote Sensing Environ.*, **22**: 432–447.

Koblinsky, C. J., J. J. Simpson and T. D. Dickey (1984), An Offshore Eddy in the California Current System, Part II: Surface manifestation, *Proc. Oceanogr.* **13**: 51–69.

Li, Jun and F. X. Zhou (1990), Computer Identification of Multispectral Satellite Cloud Imagery, *Adv. Atmos. Sci.*, **7**: 366–375.

Li, Jun and F. X. Zhou (1990), Delineation of Mesoscale Features of Ocean on Satellite IR image, *Adv. Atmos. Sci.*, **8**: 423–432.

Simpson, J. J., T. D. Dickey and C. J. Koblinsky (1984), An Offshore Eddy in the California Current System, Part I: Interior Dynamics, *Proc. Oceanogr.* **13**: 5–49.

Simpson, J. J. and R. J. Lynn (1990), A Mesoscale Eddy Dipole in the Offshore California Current, *J. Geophys.* RES.

Simpson, J. J. (1990), On the Accurate Detection and Enhancement of Oceanic Features Observed in Satellite Data, *Remote Sens. Environ.*, **33**: 17–33.

Svejkovsky, J. (1988), Sea Surface Flow Estimation from Advanced Very High Resolution Radiometer and Coastal Zone Color Scanner Satellite Imagery: a Verification Study, *J. Geophys. Res.*, **93:** 6735–6743.

Van Woert, M. (1982), The Subtropical Front: Satellite Observations During FRONTS 80, *J. Geophys. Res.*, **87:** 9523–9536.

Violette, P. E. La and R. J. Holyer (1988), Noise and Temperature Gradients in Multichannel Sea Surface Temperature Imagery of the Ocean. *Remote Sensing Environ.*, **25:** 231–241.